

Effects of Temperature on the Deposition Rate of Supersaturated Silicic Acid on Ca-type Bentonite

Tsuyoshi Sasagawa, Taiji Chida and Yuichi Niibori

Department of Quantum Science and Energy Engineering, Graduate School of Engineering, Tohoku University, Sendai 9808579, Japan

Received: August 04, 2017 / Accepted: August 14, 2017 / Published: September 30, 2017

Abstract: Na-type bentonite is commonly used as a tunnel backfilling material to prevent groundwater and radionuclide migration during the construction of a geological disposal system for high-level radioactive waste in Japan. However, host rock fractures with strong water flow can develop groundwater paths in the backfilling material. Especially, the alteration to Ca-type bentonite causes degradation of the barrier performance and accelerates the development of groundwater paths. Additionally, using cementitious materials gradually changes pH between 13 and 8. High alkaline groundwater results in high solubility of silicic acid; therefore, silicic acid is eluted from the host rock. Downstream, in the low alkaline area, the groundwater becomes supersaturated in silicic acid. This acid is deposited on Ca-type bentonite, thus leading to the clogging of the groundwater paths. In the present study, we investigate the silicic acid deposition rate on Ca-type bentonite under 288-323 K for depths greater than or equal to 500 m. The results indicate that temperature does not affect the silicic acid deposition rate up to 323 K. However, in this temperature range, the deposition of silicic acid on Ca-type bentonite in backfilled tunnels results in clogging of the flow paths.

Key words: Supersaturated silicic acid, Ca-type bentonite, backfilling material, apparent deposition rate constant, geological disposal system, flow paths.

1. Introduction

1.1 Scenario of Radionuclide Migration

In Japan, highly radioactive liquid wastes from a spent nuclear fuel processing plant that is vitrified and disposed underground at depths greater than 300 m [1]. For the immobilization of radionuclides in the geological disposal system, it is important to restrict the groundwater flow as low as possible because deep underground environments in Japan are generally filled with groundwater [1]. Therefore, for the construction of the repository, clay materials, mainly Na-type bentonite, are used as tunnel backfilling materials and buffer materials. Backfilling materials are prepared by mixing the excavated muck with Na-type bentonite [1, 2]. Bentonite is a layered silicate mineral containing

exchangeable cations (e.g., sodium, calcium, and potassium ions) in interlayers. In particular, Na-type bentonite shows various excellent properties for the retardation of radionuclide migration due to its layered structure, such as high swelling, low permeability, and adsorption of radionuclides. Conversely, when the Na ions in the bentonite interlayers are exchanged with Ca ions from the groundwater, the swelling property of the bentonite may be degraded [3]. Therefore, when the repository is groundwater saturated, the degradation of the swelling property may result in the formation of flow paths in the backfilling parts, which will increase the permeability of the groundwater. That is, the alteration to Ca-type bentonite in the backfilling parts may accelerate the migration of radionuclides.

1.2 Clogging of Flow Paths due to Silicic Acid Deposition

Now, we focus on the pH gradient in/around the

Corresponding author: Tsuyoshi Sasagawa, Ph.D. student, research fields: reaction kinetics and mass transfer.

repository, which is caused by the large amount of cementitious materials used for the construction of a geological disposal system.

As shown in Fig. 1, in the long term, alkaline species (Na, K, and Ca ions) leaching from cementitious materials increases groundwater alkalinity ($\text{pH} \approx 13$) [4]. As this highly alkaline groundwater is mixed with natural groundwater away from cementitious materials, pH gradually decreases to $\text{pH} \approx 8$ [2] (“alkaline front”). In the alkaline front, the dynamic behavior of silicic acid, which is the main component of many underground minerals, becomes complicated. Silicic acid is eluted from silicate minerals containing host rocks and engineered barriers under high alkalinity, where the silicic acid solubility is very high. Then, silicic acid deposits on the surface of the solid phase, as the liquid phase becomes supersaturated in silicic acid with decreasing solubility due to the dilution of the highly alkaline groundwater. In addition, the silicic acid excess may polymerize partially to form colloids. That is, changes in silicic acid solubility with changing pH lead to dissolution, deposition, and polymerization of silicic acid. Therefore, the dynamic behavior of silicic acid, i.e., the redistribution of silicic acid, may delay the migration of radionuclides due to the flow paths’ clogging with the deposition of silicic acid on the solid surface such as Ca-type bentonite in the backfilled tunnel. In the present study, we discuss the relationship between the silicic acid redistribution and the barrier performance in the backfilled tunnel.

The deposition of silicic acid is generally based on the following reaction formula in Fig. 2 [5].

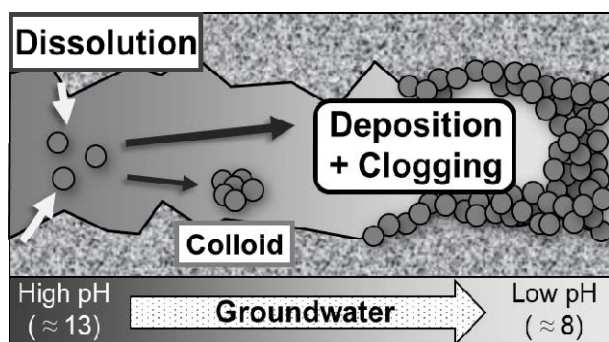


Fig. 1 Dynamic behavior of silicic acid.

Here, “M” in Fig. 2 corresponds to the component atoms (Si, Al, and so on) contained in the solid phase. As shown in Fig. 2, the deposition reaction of silicic acid is dehydration condensation. Thus, in this study, the deposition of silicic acid does not include a precipitation process, such as sedimentation of colloidal silicic acid.

1.3 Previous Studies

So far, various research studies have been performed on the underground redistribution of silicic acid in the field of geothermal science (e.g., [6]). In addition, some research results have been reported in the field of waste management. For instance, Chigira [7-9] examined the silicic acid deposition from supersaturated groundwater in the fractures of host rocks with a flow reactor. In addition, Shikazono [10] analyzed the sequential distribution of silicic-acid concentration leached from vitrified waste in/around the repository. Furthermore, Sun and Rimstidt [11] indicated that the deposition of silicic acid caused by the heating of the radioactive waste resulted in the formation of the silica cap in the Yucca mountain test site, and Matyskiela [12] observed the clogging of fractures by the deposition of silicic acid around the same site. Based on these studies, Sasagawa et al. [13, 14] estimated the apparent deposition-rate constants of supersaturated silicic acid solutions for amorphous silica experimentally, and the numerical analyses using these rate-constants showed that the deposition of silicic acid clogs the fractures of the host rock for hundreds of years. Moreover, Sasagawa et al. [15] examined the deposition behavior of silicic acid on Ca-type bentonite at room temperature (298 K). However,

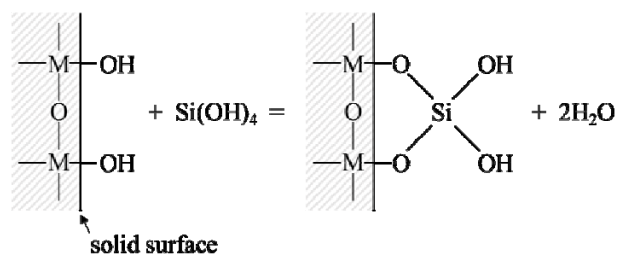


Fig. 2 Deposition reaction of silicic acid.

in general, an underground environment undergoes a geothermal gradient, which rises by approximately 3 K per depth of 100 m [16]. That is, the temperature around a repository at a depth of 500-1,000 m is estimated in the range of 303-318 K (ground level temperature is assumed to be 288 K). For understanding the redistribution of silicic acid coexisting with Ca-type bentonite in underground, it is necessary to comprehend the influence of temperature on the deposition behavior of silicic acid.

1.4 Objective of This Study

The objective of this study is to determine whether or not the redistribution of silicic acid in the repository affects the barrier performance in the backfilled tunnel after the alteration to Ca-type bentonite. Thus, our objective is to estimate the clogging effect with silicic acid deposition for flow paths formed in the backfilled tunnel considering temperature. First, we estimate the apparent deposition-rate constants by examining the dynamic behavior of silicic acid in supersaturated groundwater at temperatures up to 323 K. Next, we discuss the clogging effect for flow paths by estimating the Damköhler number based on the apparent deposition-rate constants obtained from the deposition experiments.

2. Experimental Method

2.1 Bentonite Sample

Ca-type bentonite was prepared by exchanging Na ions in the interlayer of Na-type bentonite for Ca ions. The preparation procedure for Ca-type bentonite followed the authors' previous study [17]. First, 10 g Na-type bentonite (Kunigel-VI, purchased from Kunimine Industries Co., Ltd) were stirred in 1 L 1 M CaCl_2 solution for 24 h. Then, the sample solution was left to stand for 24 h without stirring, and the supernatant solution was removed. This decantation process was repeated four times. After the ion-exchange procedure, the excess Cl, Na, and Ca ions contained in wet bentonite sample were removed

using a dialysis tube and ultra-pure water. The ion-exchanged bentonite was dried at 378 K. Finally, the Ca-type bentonite was sieved in order to retain only the particles with diameters 75 μm and less.

Exchanging Na ions with Ca ions in the bentonite interlayer was confirmed by the following measurement of the cation exchange capacity (interlayer cations) [19]. A Ca-type bentonite sample of 1 g weight was immersed in 200 mL of a solution of 0.05 M $\text{CH}_3\text{COONH}_4$ and 0.0114 M SrCl_2 . After stirring the solution with the bentonite for 1 h, the concentrations of cations (sodium, calcium, potassium, and magnesium) in the liquid phase were measured by AAS (atomic adsorption spectrometry, iCE3300, Thermo Fisher Scientific K.K., MA, USA) and ICP-AES (inductively coupled plasma atomic emission spectrometry, SPS7800, Seiko Instruments Inc., Chiba, Japan). As a result, 91.8% of the total exchangeable cations were occupied by Ca ions.

Additionally, in order to estimate the deposition-rates constants, it was important to measure the surface area contributing to the deposition of silicic acid. However, we could not confirm if silicic acid was deposited only on the surface of the bentonite particles, or it was also intercalated in the bentonite interlayer. Therefore, for comparison, we used two kinds of specific surface areas of the Ca-type bentonite for the estimation of the apparent deposition-rate constants. One is the overall specific surface area including the interlayer of Ca-type bentonite, which was estimated at 320.48 m^2/g by the EGME (ethylene glycol mono-ethyl ether) method [18]. The other is the BET (Brunauer-Emmett-Teller) specific surface area excluding the interlayer, whose value was estimated at 13.59 m^2/g using nitrogen gas.

2.2 Experimental Method for the Silicic Acid Deposition

The experiments for the deposition of silicic acid were performed by a batch reactor shown in Fig. 3, since it was important to appropriately estimate the

behavior of silicic acid in co-presence of a solid phase. The deposition experiments were performed by the following method based on the authors' previous study [15]. At the beginning, the silicic acid solution was prepared by diluting water glass (Na_2SiO_3 solution) in a polypropylene vessel. Next, Ca-type bentonite as the solid phase was poured into the silicic acid solution ($\text{pH} > 10$). Then, the deposition experiment started at the time when the pH of the solution was set to $\text{pH} = 8$ by adding a pH buffer and a HNO_3 solution. The total volume of the sample solution in these experiments was finally adjusted to 250 mL. The pH buffer was prepared by mixing THAM (tris (hydroxymethyl) aminomethane) and MES (2-morpholinoethanesulfonic acid, monohydrate).

Table 1 summarizes the parameters of the deposition experiments. As shown in Fig. 3, the supply of nitrogen gas was continued to maintain a nitrogen atmosphere for the experiments, and nitrogen gas was once moistened by a gas-washing bottle for preventing evaporation from the silicic acid solution. The deposition experiments lasted 6 h, until the deposition reaction reached approximately an apparent equilibrium

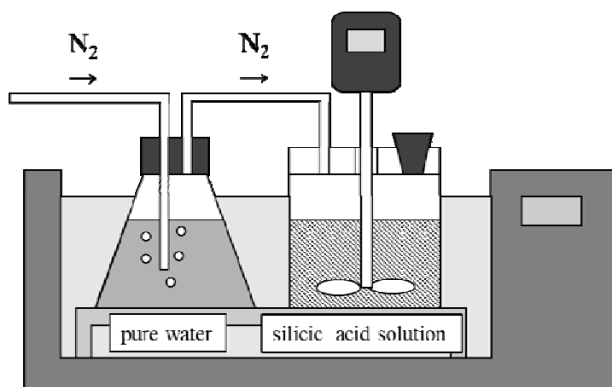


Fig. 3 Apparatus for deposition experiment.

Table 1 Experimental conditions.

| | |
|--|----------------|
| Temperature (K) | 288, 323 |
| Initial supersaturated concentrations of silicic acid (mM) | 4, 6, 8, 10 |
| Addition amount of solid sample (g) | 2.5, 5.0, 10.0 |
| pH | 8 |
| Pore size of membrane filter (μm) | 0.45 |
| Rate of stirring (rpm) | 300 |

state. Each aliquot solution collected at given time-intervals was separated into a liquid phase and a solid phase by centrifuging at 7,500 rpm for 2 min and filtrating with a 0.45- μm membrane filter. This timing of the filtration was defined as the time when the deposition reaction ended.

The supersaturation concentrations of silicic acid in Table 1 were defined by the difference between the concentration of silicic acid at the beginning of the deposition experiments and the solubility of amorphous silica. Considering the deposited material as amorphous silica, the solubility of silicic acid at $\text{pH} = 8$ was 1.62 mM at 288 K and 3.49 mM at 323 K [20, 21]. Thus, for example, when the total concentration of silicic acid at the beginning of the experiment was 5.62 mM at 288 K, the initial supersaturated concentration of silicic acid was considered 4 mM.

2.3 Measurements and Analysis of Silicic Acid

We defined the state of silicic acid as soluble silicic acid (monomeric and oligomeric), colloidal silicic acid, or deposited silicic acid, as shown in Fig. 4. The respective quantification methods were as follows.

The concentration of soluble silicic acid was quantified by the silicomolybdenum-yellow method. The concentration of colloidal silicic acid was calculated by subtracting the concentration of soluble silicic acid from the total concentration of silicic acid in the sample solution, measured with ICP-AES. The silicic acid deposited on Ca-type bentonite was calculated by subtracting the concentration of silicic

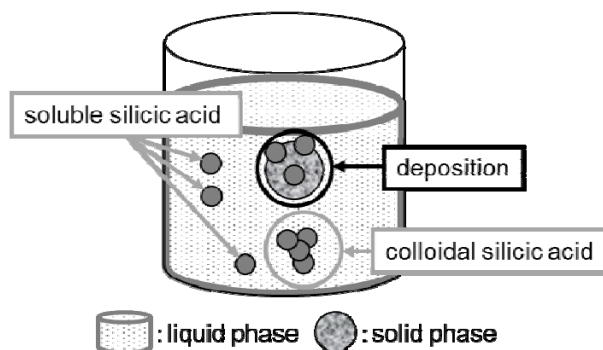


Fig. 4 Definition of silicic acid species.

acid in the sample solution (ICP-AES) from the initial concentration of silicic acid (ICP-AES) at the beginning of the experiment.

Finally, the apparent deposition-rate constants k (m/s) were estimated from the above results and the specific surface areas (m^2/g) calculated with the two methods (EGME and BET), the weight amount (g) of Ca-type bentonite, and the solution volume ($250\text{ mL} = 2.50 \times 10^{-4}\text{ m}^3$).

In addition, the particle size and the zeta potential of colloidal silicic acid in the liquid phase were measured by the dynamic light scattering method and the laser Doppler method (ELSZ-2 Plus, Otsuka Electronics Co., Ltd.), respectively. The measurements were performed as quickly as possible after the collection of the sample solution (within approximately 20 min), maintaining the temperature

of the solution by a heat-retaining function attached to this instrument. The total number of measurements for the particle size was 70, and that for the zeta potential was 10.

3. Results and Discussion

3.1 Dynamic Behavior of Silicic Acid in the Presence of Ca-Type Bentonite

Figs. 5-7 show the results of the deposition experiments at 288, 298 or 323 K; for 2.5, 5, or 10 g of Ca-type bentonite; and for initial supersaturation concentrations of 4, 6, 8, and 10 mM. The horizontal axis is time (min), and the vertical axis f is the fractions of soluble silicic acid, colloidal silicic acid, and deposition on Ca-type bentonite to the initial concentration of silicic acid. As shown in these figures,

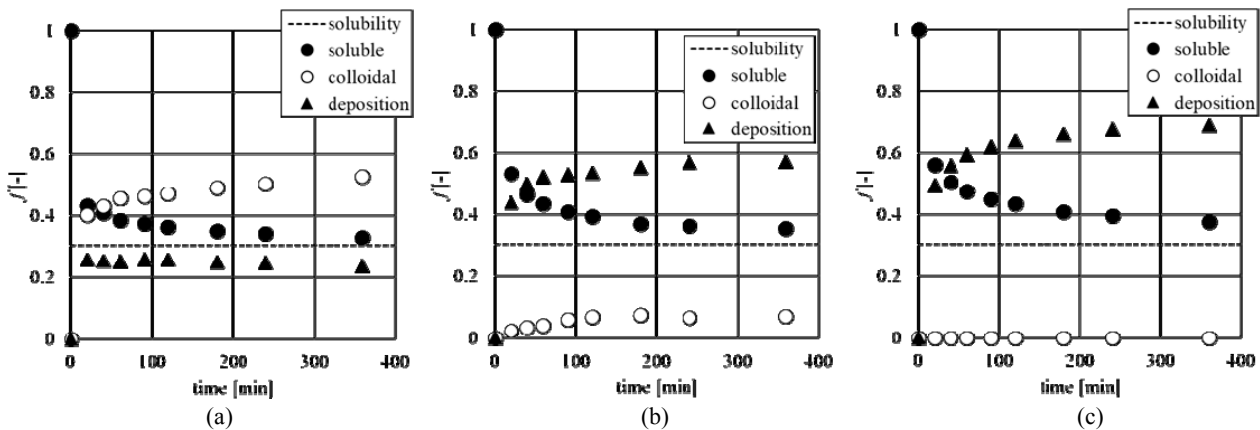


Fig. 5 Effects of amount of Ca-type bentonite on behavior of silicic acid at 323 K (initial supersaturated concentration: 8 mM, amount of solid phase: (a) 2.5 g, (b) 5.0 g, (c) 10.0 g).

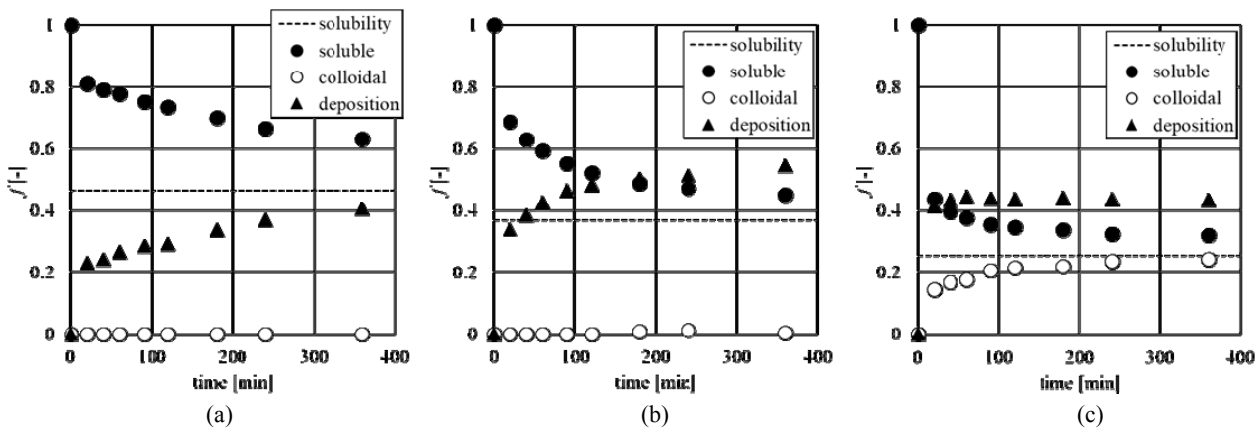


Fig. 6 Effects of initial supersaturated concentration on behavior of silicic acid at 323 K (amount of Ca-type bentonite: 5.0 g, initial supersaturated concentration: (a) 4 mM, (b) 6 mM, and (c) 10 mM).

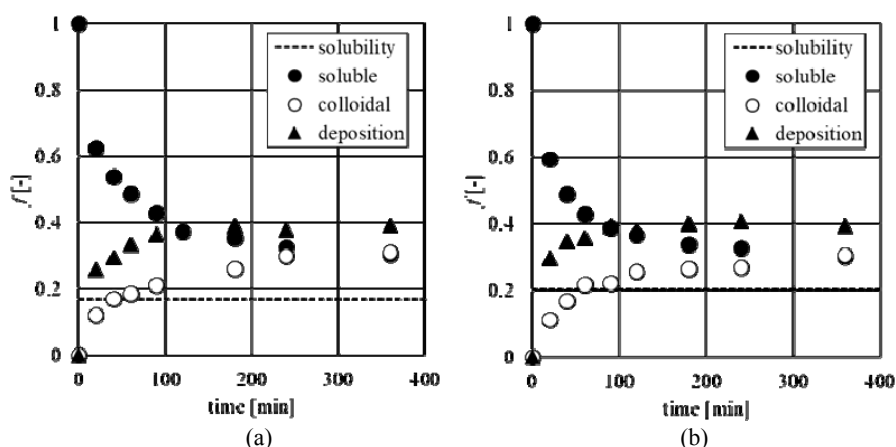


Fig. 7 Effects of temperature on behavior of silicic acid (amount of Ca-type bentonite: 5.0 g, initial supersaturated concentration: 8 mM, temperature: (a) 288 K and (b) 298 K).

the deposition of silicic acid on Ca-type bentonite increased with the concentration of soluble silicic acid under all experimental conditions. Especially, drastic deposition of silicic acid was observed within the first 20 min of the experiments. In addition, the amounts of silicic acid deposited increased with the amount of Ca-type bentonite, as shown in Fig. 5. Therefore, probably, chemically active sites on the surface of Ca-type bentonite mainly contribute to the deposition of silicic acid [22]. Conversely, significant amounts of colloidal silicic acid were formed when the amount of Ca-type bentonite was low, and the initial concentration of silicic acid was high, as shown in Figs. 5 and 6. However, considering that the underground ratio of solid phase to liquid phase is very large, the predominant reaction in the backfilled tunnels of the repository will not be based on the formation of colloidal silicic acid, but on the deposition of soluble silicic acid on the solid surface. Besides, regarding the influence of temperature, the amount of silicic acid deposited at 323 K was apparently larger than that at 288 K and 298 K, as shown in Figs. 5b and 7.

Fig. 8 shows the particle size of colloidal silicic acid in the liquid phase (8 mM of initial supersaturated concentration, and 5 g of Ca-type bentonite, 20 minutes later from the beginning of the experiments). The plots (● and □) in Fig. 8 show the mode of the particle size, and the error bars show the

size range, where 90% or more of the particles in the liquid phase are present. As shown in Fig. 8, the colloidal silicic acid observed in Figs. 5-7 was around 100 nm in size. Moreover, the particle size was not affected by the formation and depolymerization of colloidal silicic acid at 288-323 K, and within the time of these experiments.

Fig. 9 shows the zeta potential of colloidal silicic acid under the same conditions as Fig. 8, which also shows similar values for 288 K and 323 K. That is, the particle size and the zeta potential of colloidal silicic acid in the experiments were not affected by temperature in the range of 288-323 K. In general, the aggregation and precipitation of colloidal species progress with absolute values lower than the zeta potential

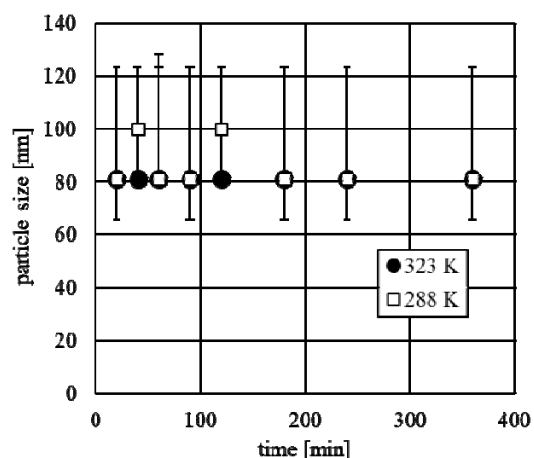


Fig. 8 Particle size (supersaturated silicic acid concentration 8 mM, weight of solid phase 5.0 g).

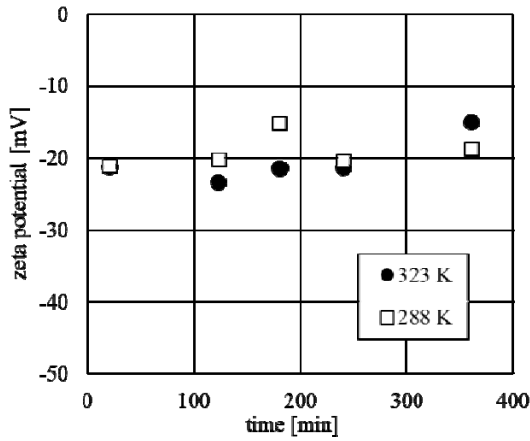


Fig. 9 Zeta potential (supersaturated silicic acid concentration 8 mM, weight of solid phase 5.0 g).

shown in Fig. 9 (e.g., [5]). Therefore, colloidal silicic acid left in the liquid remained stable at least for 6 hr in this study. However, the aggregation and precipitation of colloidal silicic acid might contribute to the clogging effect of flow-paths for the long term at higher temperatures in the deep underground, even if colloidal silicic acid temporarily forms in the flow paths.

3.2 Estimation of Apparent Deposition-Rate Constant

Based on the results of the deposition experiments, we estimate the apparent deposition-rate constant k (m/s). Here, as shown in Eqs. (1)-(4), the concentrations of soluble silicic acid, colloidal silicic acid, and deposited silicic acid are expressed as fractions of the initial concentration of silicic acid, as shown below:

$$f = \frac{c_f}{c_{ini}} \quad (1)$$

$$f_c = \frac{c_c}{c_{ini}} \quad (2)$$

$$f_d = \frac{c_d}{c_{ini}} = 1 - f - f_c \quad (3)$$

$$f_e = \frac{c_e}{c_{ini}} \quad (4)$$

where c_f , c_c , and c_d are the concentrations of soluble silicic acid, colloidal silicic acid, deposition of silicic acid (mM), respectively. c_e is the solubility of

amorphous silica (mM); c_{ini} is the initial concentration of silicic acid (mM); and f , f_c , f_d , and f_e are the fractions of the concentration of soluble silicic acid, colloidal silicic acid, deposited silicic acid, and solubility to initial concentration of silicic acid. Then, the changes in the concentrations of soluble silicic acid and colloidal silicic acid per unit time are described by Eqs. (5)-(7).

$$-\frac{df}{dt} = kA(f - f_e) + k_c^+(f - f_e)^n - k_c^-f_c^m \quad (5)$$

$$A = \frac{aM}{V} \quad (6)$$

$$\frac{df_c}{dt} = k_c^+(f - f_e)^n - k_c^-f_c^m \quad (7)$$

where t is time (s), k is the apparent deposition-rate constant (m/s), and A is the surface area (1/m) based on the amount of Ca-type bentonite. Then, a is the specific surface area (m²/g), M is the amount of Ca-type bentonite, V is the liquid phase volume (m³), k_c^+ and k_c^- are the polymerization and the depolymerization rate-constants of colloidal silicic acid (1/s), and n and m refer to the reaction order. The change in the deposition of silicic acid per unit time is summarized as Eq. (8) by using Eqs. (1), (5), and (7).

$$\frac{df_d}{dt} = \frac{d(1 - f - f_c)}{dt} = -\frac{df}{dt} - \frac{df_c}{dt} = kA(f - f_e) \quad (8)$$

Finally, Eq. (9) is obtained by substituting $f = 1$ at $t = 0$ in Eq. (8).

$$r_{ini} = \left. \frac{df_d}{dt} \right|_{ini} = kA(1 - f_e) \quad (9)$$

where r_{ini} is the initial deposition rate (1/s), which is obtained from the gradient (at $t = 0$) of a quadratic curve based on initial three plots of deposition data. Moreover, r_{ini} is calculated through two methods in order to consider the initial drastic change in the deposition of silicic acid. Hereinafter, the two methods are referred to as Case (A) and Case (B). "Case (A)" includes the point $f_d = 0$ at $t = 0$ for the calculation of r_{ini} , and "Case (B)" excludes the point $f_d = 0$ at $t = 0$.

These r_{ini} values are calculated considering the surface area of the solid phase, as shown in Eq. (9). In this study, after the values of r_{ini} are calculated for 2.5, 5, and 10 g Ca-type bentonite, the apparent deposition-rate constants k (m/s) based on Eq. (9) are estimated from the correlation of r_{ini} and A defined by Eq. (6). For the specific surface area a , the EGME method gives 320.48 m²/g, and the BET method give 13.59 m²/g.

Table 2 shows the apparent deposition-rate constants k calculated from the experimental results and Eq. (9). The values of k for 298 K are calculated by referring to the results of author's previous study [15]. As shown in Table 2, the k values for 13.59 m²/g specific surface area are one order of magnitude or more larger than those for 320.48 m²/g. Concerning the difference between Case (A) and Case (B), most of the k values estimated for the condition of Case (A) exceed those of Case (B), and the range of k for Case (B) is apparently wide in comparison with those for Case (A). As shown in the results of the deposition experiments (Figs. 5-7), the gradients of the deposition amount in the time range from 0 to 40 minutes for Case (A) seriously exceed those for Case (B) in the time range from 20 to 60 minutes. This means that the decrease of the surface area is caused by the deposition of silicic acid relatively early in the experiments.

In this present study, the apparent deposition-rate constants are evaluated in consideration of the surface areas measured by the EGME method and the BET (N₂ gas) method. In the results, almost the same apparent deposition-rate constants are obtained in the range of 10⁻¹²-10⁻¹¹ m/s for 320.48 m²/g and 10⁻¹¹-10⁻⁹ m/s for 13.59 m²/g. In particular, these values of k for Case (A) converge within the range of one order of magnitude. Besides, the initial supersaturation concentration of silicic acid scarcely affects the apparent deposition-rate constants. Note that the rate-constant in Eq. (9) is essentially independent of the initial supersaturation concentration.

Furthermore, as shown in Table 2, the change in temperature hardly influences the apparent deposition-rate constants. In order to compare those quantitatively, the apparent activation energy (kJ/mol) based on the Arrhenius' plot is estimated using the k values of Case (A) in Table 2. Table 3 shows the apparent activation energy calculated from Table 2. As a result, these values of the apparent activation energy are very low. These results suggest that the deposition of silicic acid on Ca-type bentonite is limited not only by the chemical reaction, as shown in Fig. 2, but also by some diffusion processes, e.g., the diffusion of silicic acid into the interlayer of Ca-type bentonite.

Table 2 Apparent deposition-rate constant k (m/s).

| Specific surface area | Temperature | Case | Initial supersaturated concentration of silicic acid | | | |
|---|-------------|------|--|--------------------------|--------------------------|--------------------------|
| | | | 4 mM | 6 mM | 8 mM | 10 mM |
| 320.48 m ² /g (EGME method) | 288 K | (A) | 4.20 × 10 ⁻¹¹ | 2.00 × 10 ⁻¹¹ | 2.41 × 10 ⁻¹¹ | 3.73 × 10 ⁻¹¹ |
| | | (B) | 6.14 × 10 ⁻¹² | 2.16 × 10 ⁻¹² | 1.09 × 10 ⁻¹¹ | 6.74 × 10 ⁻¹² |
| | 298 K [15] | (A) | 2.28 × 10 ⁻¹¹ | 3.63 × 10 ⁻¹¹ | 3.72 × 10 ⁻¹¹ | 5.30 × 10 ⁻¹¹ |
| | | (B) | 3.11 × 10 ⁻¹² | 5.12 × 10 ⁻¹³ | 3.83 × 10 ⁻¹² | 3.86 × 10 ⁻¹² |
| | 323 K | (A) | 3.85 × 10 ⁻¹¹ | 3.60 × 10 ⁻¹¹ | 3.64 × 10 ⁻¹¹ | 6.49 × 10 ⁻¹¹ |
| | | (B) | 2.36 × 10 ⁻¹² | 3.11 × 10 ⁻¹² | 2.12 × 10 ⁻¹¹ | 4.16 × 10 ⁻¹² |
| 13.59 m ² /g (BET method) | 288 K | (A) | 9.92 × 10 ⁻¹⁰ | 4.72 × 10 ⁻¹⁰ | 5.68 × 10 ⁻¹⁰ | 8.79 × 10 ⁻¹⁰ |
| | | (B) | 1.45 × 10 ⁻¹⁰ | 5.10 × 10 ⁻¹¹ | 2.58 × 10 ⁻¹⁰ | 1.59 × 10 ⁻¹⁰ |
| | 298 K [15] | (A) | 5.39 × 10 ⁻¹⁰ | 8.55 × 10 ⁻¹⁰ | 8.76 × 10 ⁻¹⁰ | 1.25 × 10 ⁻⁹ |
| | | (B) | 7.34 × 10 ⁻¹¹ | 1.20 × 10 ⁻¹¹ | 9.04 × 10 ⁻¹¹ | 9.10 × 10 ⁻¹¹ |
| | 323 K | (A) | 9.08 × 10 ⁻¹⁰ | 8.51 × 10 ⁻¹⁰ | 8.59 × 10 ⁻¹⁰ | 1.53 × 10 ⁻⁹ |
| | | (B) | 5.55 × 10 ⁻¹¹ | 7.34 × 10 ⁻¹¹ | 4.99 × 10 ⁻¹⁰ | 9.81 × 10 ⁻¹¹ |

Table 3 Apparent activation energy (kJ/mol).

| Initial supersaturated concentration (mM) | 4 | 6 | 8 | 10 |
|---|-----|-------|------|-------|
| Apparent activation energy (kJ/mol) | 1.2 | 10.77 | 7.47 | 11.27 |

3.3 Damköhler Number

As a reasonable index, we use the Damköhler number for the estimation of the deposition effect of silicic acid on Ca-type bentonite; the Damköhler number is a non-dimensional number referring to chemical processes, which takes into consideration for example the deposition rate of silicic acid to the mass-transport rate including the groundwater flow, and it is calculated by Eq. (10), as follows,

$$D_a = \frac{xa_1k}{u} \quad (10)$$

where, D_a is the Damköhler number, x is the characteristic length (m), and u is the groundwater flow rate (m/s). In this study, the parameters are set as follows: $x = 5$ (m) assuming the diameter of tunnels [1], $u = 0.5$ (m/y) [1], and $k = 10^{-12}$ (m/s) as obtained in this study. The specific surface area per unit volume, a_1 , is the product of the apparent specific gravity 0.6 g/cm^3 and the specific surface area per unit mass, $a = 13.59 \text{ m}^2/\text{g}$. These values of the parameters are selected conservatively so that, when the Damköhler number becomes smaller, the deposition of silicic acid is lower.

As a result, the Damköhler number values are estimated as 10^2 or more for all apparent deposition-rate constants. This means that the silicic acid deposition on Ca-type bentonite is largely determined by the groundwater flow, and the flow-paths in backfilled tunnels are efficiently clogged.

4. Conclusions

We estimated the apparent deposition-rate constant k (m/s) for Ca-type bentonite quantitatively, considering the effect of temperature around the repository. In addition, the clogging effect with the deposition of silicic acid in the flow-paths was discussed by using the Damköhler number.

In the deposition experiments, the deposition amount of silicic acid increased seemingly due to the

growing of colloidal silicic acid at high temperature experiments (323 K) in the case of relatively smaller in amount of Ca-type bentonite. The estimated apparent deposition-rate constant differed by more than one order of magnitude depending on the specific surface area ($320.48 \text{ m}^2/\text{g}$ by EGME method or $13.59 \text{ m}^2/\text{g}$ by BET method) and/or on whether $f_d = 0$ at $t = 0$ or not. Conservative values from these were about 10^{-12} m/s in the experiments of specific surface area $320.48 \text{ m}^2/\text{g}$ and Case (B) (excluding $f_d = 0$). Additionally, the calculated apparent activation energy to estimate the effects of temperature was sufficiently small. That is, the deposition reaction of silicic acid on Ca-type bentonite was not significantly affected by temperature in the range of 288-323 K. Finally, the Damköhler number for an apparent deposition-rate constant of 10^{-12} m/s exceeded 10^2 . This means that the deposition of silicic acid is sufficiently fast in comparison with the groundwater flow rate around the repository. Therefore, these results suggest that the flow paths will be clogged by the deposition of silicic acid on Ca-type bentonite in a high temperature environment (323 K) such as a deep underground environment, even if the flow paths are developed in backfilled tunnels. As a future work, the temporal and spatial redistribution of silicic acid in backfilled tunnels should be clarified by the numerical mass-transport simulation using the apparent deposition-rate constant and a flow experiment simulating an actual environment.

Acknowledgements

This work supported by JSPS KAKENHI, Grant-in-Aid for Young Scientists (B) No. 16K18345 and Grant-in-Aid for JSPS Fellows No. 16J02619.

References

- [1] JNC (Japan Nuclear Cycle development institute). 1999. H12 Project to Establish the Scientific and Technical Basis for HLW Disposal in Japan, Supporting Report II,

- Repository Design and Engineering Technology. JNC, Japan, JNC TN1400 99-021.
- [2] Japan Nuclear Cycle Development Organization Institute and the Federation of Electric Power Companies of Japan. 2005. Second Progress Report on Research and Development for TRU Waste Disposal in Japan. JNC and FEPC, Japan, JNC-TY1400-2005-013.
- [3] Mihara, M. 2000. "The Comparison Concerned with Hydraulic Conductivities and Effective Diffusion Coefficients for Nuclides between Na and Ca Bentonite." *JNC Technical Review* 6 (3): 61-8.
- [4] Atkinson, A. 1985. "The time Dependence of pH within a Repository for Radioactive Waste Disposal," *United Kingdom Atomic Energy Authority, AERE-R 11777*.
- [5] Iler, R. K. 1979. *The Chemistry of Silica-Solubility, Polymerization, Colloid and Surface Properties, and Biochemistry*. New York: John Wiley & Sons.
- [6] Rimstidt, J. D., and Barnes, H. L. 1980. "The Kinetics of Silica-Water Reactions." *Geochimica et Cosmochimica Acta* 44 (11): 1683-99.
- [7] Chigira, M. 1991. "Sealing of Rock Fractures Around HLW Repositories (Part 1)—A New Hydrothermal Fracture Flow Apparatus and Its Preliminary Application to Self-sealing by Silica." *CRIEPI Research Report, U91031* [in Japanese].
- [8] Chigira, M. 1993. "Sealing of Rock Fractures around HLW Repositories (Part 2)—Silica Precipitation Behavior in Flow Fields." *CRIEPI Research Report, U92050* [in Japanese].
- [9] Chigira, M. 1996. "Sealing of Rock Fractures around HLW Repositories (Part 3)—Silica Precipitation Rate, Colloidal Formation, and Pore Closure." *CRIEPI Research Report, U95053* [in Japanese].
- [10] Shikazono, N. 1995. *Radioactive Waste and Geoscience*. Tokyo: Tokyo University Press.
- [11] Sun, Z., and Rimstidt, J. D. 2002. "Silica Transport in the High-Level Radioactive Waste Repository, Yucca Mountain, Nevada." *Environmental & Engineering Geoscience* 8 (1): 3-9.
- [12] Matyskiela, W. 1997. "Silica Redistribution and Hydrologic Changes in Heated Fractured Tuff." *Geology* 25 (12): 1115-8.
- [13] Sasagawa, T., Chida, T., Niibori, Y., and Mimura, H. 2015. "Effects of pH on Deposition Rate of Supersaturated Silicic Acid around Geological Disposal System." *Proc. of WM 2015, Arizona*, March 15-19, 2015, Paper No. 15245.
- [14] Sasagawa, T., Chida, T., Niibori, Y., and Mimura, H. 2015. "Effects of Supersaturated Silicic Acid Concentration on Deposition Rate around Geological Disposal System." *Proc. of ICONE23, Chiba*, May 17-21, 2015, Paper No. ICONE23-1223.
- [15] Sasagawa, T., Chida, T., and Niibori, Y. 2016. "Deposition Behavior of Supersaturated Silicic Acid on Ca-Type Bentonite in Geological Disposal System." *Proc. of WM 2016, Arizona*, March 6-10, Paper No. 16033.
- [16] JNC (Japan Nuclear Cycle Development Institute). 1999. H12 Project to Establish the Scientific and Technical Basis for HLW Disposal in Japan, Supporting Report I, Geological Environment in Japan. JNC, Japan, JNC TN1400 99-021.
- [17] Kozaki, T., Fujishima, A., Sato, S., and Ohashi, H. 1997. "Self-diffusion of Sodium Ions in Compacted Sodium Montmorillonite." *Nuclear Technology* 121 (1): 63-9.
- [18] Eltantawy, M., and Arnold, P.W. 1973. "Reappraisal of Ethylene Glycol Mono-Ethyl Ethel (Egme) Method for Surface Area Estimations of Clays." *Journal of Soil Science* 24 (2): 232-8.
- [19] Japanese Society of Soil Science and Plant Nutrition. 1997. *The Analysis of Soil Environment*, Hakuyusha Co., Ltd., Tokyo.
- [20] Berner, R. A. 1971. *Principles of Chemical Sedimentology*. New York: McGraw-Hill.
- [21] Lindsay, W. L. 1979. *Chemical Equilibria in Soils*. New York: John Wiley & Sons.
- [22] Hombøe, M., Wold, S., and Petterson, T. 2011. "Effects of the Injection Grount Silica Sol on Bentonite." *Physics and Chemistry of the Earth* 36 (17-18): 1580-9.